Multiple frequency response points identification through single asymmetric relay feedback experiment ⋆

Oscar Miguel-Escrig [a], Julio-Ariel Romero-Pérez [a], José Sánchez-Moreno [b], Sebastián Dormido [b]

[a] *Department of System Engineering and Design. Universitat Jaume I (UJI). Castelló de la Plana.*

[b] *Department of Computer Science and Automatic Control. Universidad Nacional de Educación a Distancia (UNED). Madrid.*

Abstract

In this paper a methodology to identify several points of the frequency response of a system using a single experiment is proposed. The identification is performed using the information obtained from an asymmetric relay feedback experiment. The frequency response points that are estimated correspond to the fundamental oscillation frequency induced by the asymmetric relay and its harmonics. The method is easy to implement since it only requires linear algebra operations, but relies on a proper data selection, which is largely studied, to obtain the most accurate results. The proposed method allows a Least Squares formulation, which has also been studied, and presents some benefits in terms of accuracy for certain cases. The presented results are validated experimentally using a practical identification case.

Key words: system identification, relay experiment, Fourier series.

1 Introduction

Among the system identification tools that have been developed in the domain of control engineering, relay-feedback identification method can be found as one of the most used and studied. One of the firsts works presenting a relay-feedback experiment can be found in [12], but it was not until mid 80s when the main ideas regarding the relay-feedback identification were further developed in [1].

Successive improvements have been done from the original idea [18,20], however, most of the published works use the Describing Function (DF) method [13] as the analysis tool. The DF method allows obtaining the ultimate gain, the ultimate frequency and the phase lag of the process with a simple harmonic analysis [8].

Some works have been conducted aiming to extract more information from the system using this basis. Such works usually require either to extend the duration of the experiments or to modify the loop structure to a different extent. For example, several works modify the relay setup to obtain oscillation frequencies lower than the ultimate frequency, to that end, different strategies can be implemented, for instance including time delays in the loop [16,17,30], inserting an integrator [7,33,39], modifying the hysteresis of the relay [18] or modifying the vertical asymmetry [11].

Other works are focused on improving the degree of accomplishment of the filtering hypothesis that the DF technique assumes. This is attained by modifying the loop structure to induce more sinusoidal-like oscillations, using for instance a pre-load relay [35], a saturation relay [40], adding more levels at the output of the relay [34], or using a mapping function to the relay output [15]. Other authors propose schemes with multiple relays [6], or substituting the relay by a Symmetric-Send-On-Delta (SSOD) non-linearity [26].

However, there exist other lines of research which use analysis techniques others than the Describing Function. The usage of such tools generally produces more accurate results at the expense of requiring more time to be obtained. Some of these methods are based on the

⋆ This paper was not presented at any IFAC meeting. Corresponding author O. Miguel-Escrig Tel. +34964729124. e-mail: omiguel@uji.es

Email addresses: omiguel@uji.es (Oscar Miguel-Escrig), romeroj@uji.es (Julio-Ariel Romero-Pérez), jsanchez@dia.uned.es (José Sánchez-Moreno), sdormido@dia.uned.es (Sebastián Dormido).

Fourier transform [4,5,37], another work defines the A-locus to identify low order systems [10], and others propose to take into account the effect of harmonics in the response [14]. Other authors also consider the shape of the induced oscillation for the identification procedure [21,36]. Other works like [2,3] relate the characteristics of the temporal response of an asymmetric relay experiment with the parameters of FOPTD and IPTD models by using the inverse Laplace transform. Another approach, called the 2-shifting method was described in [9], which allows obtaining 2 points of the frequency response. This method has been further developed resulting in the n-shifting method which has been used to identify n points instead [27,28]. Certainly, there exist other approaches to the identification problem, for example the one presented in [38], which proposes to replace the traditional relay by a parasitic relay or a cascade relay. These kinds of approaches improve the identification results, but add complexity to the procedure.

All in all, there are a wide range of alternatives to improve the identification results with regard to the original idea, however, most of them require either to expand the duration of the experiments, introduce modifications or further elements on the loop, or involve more complicated calculations which could be a problem for the practical application of the methodology.

One of the paramount virtues of the relay feedback experiment is its simple setup. Some of the aforementioned works present different degrees of variation with regard to the relay structure, among these works, the variation presented in [28], which is a fully asymmetric and delaying relay, named FAD relay for short, can provide flexibility without compromising the difficulty of the setup. The FAD relay contains biases in its detection and in its output, and some user-defined delay to its output, which as it was shown in [28] allows decreasing the fundamental oscillation frequency, being, thus, possible to identify regions of the frequency response below the ultimate frequency. The information provided by this region is of interest, for example, for tuning PID controllers.

In this paper, the concepts and methodology for identification developed in [22] will be applied to the asymmetric relay, which is the simplest version of the FAD relay. The proposal allows obtaining several points of the frequency response with the information gathered from only one sustained oscillation. Unlike other methods, this approach does not increase the duration of the experiments to obtain several points of the frequency response, overcoming the necessity of repeating several feedback relay experiment with different delays for obtaining them. With the obtained points, it can then be obtained a parametric transfer function using any of the methods presented in [23] to tune a controller or directly use a tuning method that can be applied to non-parametric models like [29]. The obtained results are directly applicable to any auto-tuning method that requires several frequency response points [25].

Besides, it is shown that with a proper selection of the samples accurate estimations are obtained without involving complicated calculations. These samples, which are expressed as fractions of the oscillation period, are selected according to calculus criteria, and therefore, they do not depend on the shape of the oscillation. Those time fractions are always the same and can be directly selected once the period of the induced oscillation is known. Unlike the results presented in [22], where an ideal relay is used, the characteristics of the asymmetric relay allows obtaining sustained oscillation with harmonic content in both odd and even harmonics, allowing to estimate more points of the frequency response in the region of interest. In addition, it is shown that some induced oscillations are suitable to identify until a certain number of points in the frequency domain.

The result of the identification procedure presented in this paper is a non-parametric model in the frequency field. However, unlike the standard methods for obtaining this kind of models, which use the Fourier transform of the input and output signals, the proposed method relies on the use of the Fourier series. This is possible due to the periodic response of the system under relay feedback experiment. This fact avoids some issues related with the calculation of the Fourier transform of aperiodic signals, as the leakage error [31]. The results of the method are affected by the truncation of the Fourier series and for the measurement error, whose effects have been addressed in the paper.

The paper is organized as follows. In Section 2, the loop setup for identification as well as the main elements involving the identification procedure are presented. Section 3 details the main results obtained and proposes the guidelines to perform the identification. In Section 4 the proposed method is applied to several case studies. Section 5 describes the effect of noise on the identification procedure. In Section 6 the applicability of the proposed identification method is evaluated following a Least Squares approach. Then, an experimental case is addressed in Section 7. Finally, the conclusions about this work are drawn in Section 8.

2 Problem statement

Consider the block diagram of a loop with an asymmetric relay as it is shown in Figure 1, where y_r, $e(t)$, $u(t)$ and $y(t)$ are the reference, error, relay output and measured output signals respectively. In this diagram, the process to identify is denoted by $G(s)$ and the asymmetric relay with its own block. The asymmetric relay considered has u_A and u_B as upper and lower drive levels, and e_A and e_B as upper and lower switch points. The relationship between the input signal e and the output signal u for

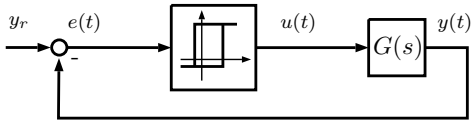

Fig. 1. Set up for the identification with an asymmetric relay.

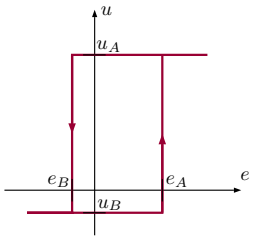

Fig. 2. Input-Output relationship for the asymmetric relay.

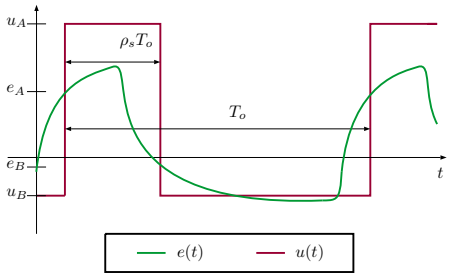

Fig. 3. Generic oscillation waveform for a system with an asymmetric relay.

the asymmetric relay is depicted in Figure 2. An example oscillation is presented in Figure 3, where the error signal $e(t)$ and the relay output $u(t)$ are shown. The error signal is quantized by the relay according to the commutation thresholds e_A and e_B resulting in the output signal $u(t)$. This signal switches from u_A to u_B, which correspond to the relay drive levels, at the commutation time $\rho_s T_o$, being T_o the oscillation period and ρ_s the time fraction where the switch is produced.

The relay feedback experiments for identification use the sustained oscillations induced by the relay to obtain information about the process to identify. Most of classical approaches are focused on identifying the ultimate oscillation point, which corresponds to the point where the phase of $G(s)$ is $-180°$. While the information provided by this point is useful, for instance for tuning PID controllers, it does not provide any information about the low frequency response of the process, which can play an important role in the behavior of the closed-loop response of the controlled system.

The goal of this paper is to perform a relay feedback identification experiment with the asymmetric relay and provide an estimation of those points of the frequency response of the process whose frequency corresponds to the oscillation frequency and its multiples, also called harmonics. This kind of identification procedure has been developed in [22] for the relay feedback experiment, and some of those ideas are extended to the asymmetric relay case.

To start with the identification procedure, the relay output signal $u(t)$, depicted in Figure 3, is obtained whose expression corresponds to (see Appendix A):

$$u(\tau T_o) = \rho_s(u_A\text{-}u_B) + u_B + \frac{2(u_A\text{-}u_B)}{\pi}\sum_{n=1}^{\infty}\frac{1}{n}\sin(\pi n\rho_s)\cos(\pi n(2\tau\text{-}\rho_s)) \tag{1}$$

where the time variable has been expressed as a product of the oscillation period T_o and a time fraction $\tau \in [0, 1]$.

This expression is used to compute the measured output of the system $y(t)$, which is presented in equation (2), and includes the gain of the process $G(0)$ and is a function of the real and imaginary parts of the oscillation frequency ω_o and its harmonics $\omega_n = n\omega_o$.

For the identification procedure presented, it is assumed that the system gain $G(0)$ is known. There exist several methods to identify it, for example, with a step response experiment around the operation point or using the output of a biased relay as shown in [19,32]:

$$G(0) = -\frac{\int_0^{2\pi} e(t)d\omega t}{\int_0^{2\pi} u(t)d\omega t}. \tag{3}$$

This last method may result more convenient due to the usage of an asymmetric relay.

At this point, equation (2) is expressed as a linear equation where the information related to the process, which is gathered in the real and imaginary parts of each harmonic, is to be determined. Using this equation, a study about its use for the estimation of the frequency response points of $G(s)$ is presented in the following sections.

3 Main result

Regarding to equation (2), under the identification of processes perspective, the real and imaginary parts of the process are seen as unknown quantities. Furthermore, focusing on the summation, for each harmonic n considered in that summation, two unknowns are added, which are the real and imaginary part of that particular harmonic. For example, to calculate the real and imaginary part of the fundamental frequency, a system of equations formed by two instances of equation (2) with different values of τ would be needed at least. If an additional harmonic wants to be computed, then 4 unknowns

$$y(\tau T_o) = [\rho_s(u_A - u_B) + u_B]\, G(0) + \frac{2(u_A - u_B)}{\pi} \sum_{n=1}^{\infty} \frac{1}{n} \sin(\pi n \rho_s) \left[\Re\{G(j\omega_n)\} \cos(\pi n(2\tau - \rho_s)) - \Im\{G(j\omega_n)\} \sin(\pi n(2\tau - \rho_s))\right] \quad (2)$$

appear, needing at least 4 equations. Generally speaking, to compute the first n harmonics a number of equations $l \geq 2n$ is needed. Thus, the system of equations to solve can be formulated generally as:

$$Y_{l\times 1} = \bar{Y}_{l\times 1} + \frac{2(u_A - u_B)}{\pi} A_{l\times 2n} B_{2n\times 2n} S_{2n\times 1}, \quad (4)$$

where each of the presented elements is described in equations (5) and (6), where $\mathbf{1}$ is a $l \times 1$ column vector in which every element is equal to 1. Therefore, the frequency response points of the process contained in S, considering $l = 2n$, can be obtained by computing:

$$S = \frac{\pi}{2(u_A - u_B)} (AB)^{-1} (Y - \bar{Y}). \quad (7)$$

In any linear system, the matrix to invert can strongly influence the accuracy of the obtained solution, which in this case, is the matrix AB. Regarding to each of these matrices separately, it can be seen that they mainly depend on the commutation time fraction ρ_s and on the time fractions of the different samples taken τ_i. Hence, the value of samples taken, gathered in Y, do not have an impact on the accuracy of the solution, being the commutation time and the choice of the samples taken the paramount parameters that determine the accuracy of the obtained solution.

The structure of these matrices, allow pre-calculating the values of ρ_s and τ_i that lead to the most accurate solution. This choice is important since some combinations of values of τ_i could lead to a linear dependent system of equations or to some systems of equations where two equations are very similar. To illustrate this fact, consider a simple case where $n = 3$, the samples τ_i are chosen evenly spaced as follows:

$$\tau_i = \left[0,\ \frac{1}{6},\ \frac{2}{6},\ \frac{3}{6},\ \frac{4}{6},\ \frac{5}{6}\right],$$

and for illustrative purposes let us consider $\rho_s = 1/3$. The matrix A according to expressions in (5) results in:

$$A = \begin{bmatrix} 0.5 & -0.5 & -1 & 0.866 & 0.866 & 0 \\ 1 & 1 & 1 & 0 & 0 & 0 \\ 0.5 & -0.5 & -1 & -0.866 & -0.866 & 0 \\ -0.5 & -0.5 & 1 & -0.866 & 0.866 & 0 \\ -1 & 1 & -1 & 0 & 0 & 0 \\ -0.5 & -0.5 & 1 & 0.866 & -0.866 & 0 \end{bmatrix}.$$

As it can be seen, all the elements of the last column of this matrix are zeros, which makes A not invertible, making this choice of the sample times τ_i not suitable for the identification.

Besides, choosing a set of τ_i according to any arbitrary sampling pattern could also lead to a linear system in which small errors in the measured signal, due to noise for instance, could lead to a significant loss in the accuracy of the final solution.

This accuracy or sensitivity of the solution is measured by the condition number $\kappa(\cdot)$ which can be computed as:

$$\kappa(\cdot) = \|\cdot\| \left\|\cdot^{-1}\right\|$$

where the operator $\|\cdot\|$ denotes the matrix norm. For the calculations in this work, it is considered the euclidean condition number, obtained with the euclidean norm.

With regard to the condition number of AB the following expression can be used:

$$\kappa(AB) \leq \kappa(A)\kappa(B)$$

which allow defining an upper bound for the condition number of AB by computing the condition number of each of them. This is specially useful since matrix B is more dependent on the running experiment, because it depends on the asymmetry of the induced oscillation, and matrix A mostly depends on the choice of the samples τ_i. In addition, by computing them separately the analysis results easier and enlightening.

3.1 Characterizing $\kappa(B)$

Regarding to B, since it is a normal matrix ($BB^T = B^TB$), its condition number can be computed as:

$$\kappa(B) = \frac{|\lambda_{max}(B)|}{|\lambda_{min}(B)|}, \quad (8)$$

being $\lambda_{max}(B)$ and $\lambda_{min}(B)$ the maximum and minimum eigenvalues of B. Since B is a diagonal matrix, its eigenvalues are the elements of the diagonal, resulting in the condition number of B to be expressed as:

$$\kappa(B) = \frac{\max\limits_{1\leq i\leq n} |\sin(i\pi\rho_s)/i|}{\min\limits_{1\leq i\leq n} |\sin(i\pi\rho_s)/i|}. \quad (9)$$

$$Y = \begin{bmatrix} y(\tau_1 T_o) \\ y(\tau_2 T_o) \\ ... \\ y(\tau_l T_o) \end{bmatrix}, \quad A = \begin{bmatrix} \cos(\pi(2\tau_1 - \rho_s)) & ... & \cos(n\pi(2\tau_1 - \rho_s)) & -\sin(\pi(2\tau_1 - \rho_s)) & ... & -\sin(n\pi(2\tau_1 - \rho_s)) \\ \cos(\pi(2\tau_2 - \rho_s)) & ... & \cos(n\pi(2\tau_2 - \rho_s)) & -\sin(\pi(2\tau_2 - \rho_s)) & ... & -\sin(n\pi(2\tau_2 - \rho_s)) \\ ... & & ... & ... & & ... \\ \cos(\pi(2\tau_l - \rho_s)) & ... & \cos(n\pi(2\tau_l - \rho_s)) & -\sin(\pi(2\tau_l - \rho_s)) & ... & -\sin(n\pi(2\tau_l - \rho_s)) \end{bmatrix}, \quad (5)$$

$$B = diag\left(\sin(\pi\rho_s), ..., \frac{\sin(n\pi\rho_s)}{n}, \sin(\pi\rho_s), ..., \frac{\sin(n\pi\rho_s)}{n}\right), \; \bar{Y} = [\rho_s(u_A\text{-}u_B)+u_B]\, G(0)\mathbf{1} \text{ and } S = \begin{bmatrix} \Re\{G(j\omega_o)\} \\ ... \\ \Re\{G(jn\omega_o)\} \\ \Im\{G(j\omega_o)\} \\ ... \\ \Im\{G(jn\omega_o)\} \end{bmatrix}. \quad (6)$$

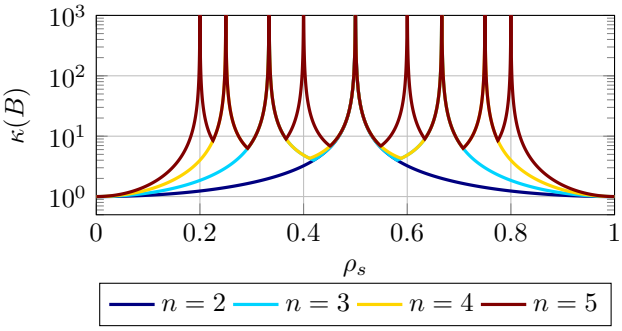

Fig. 4. Condition number $\kappa(B)$ for all the values of ρ_s and considering different harmonics.

Since the denominator can be made 0 for some combinations of ρ_s and i there exist several combinations of ρ_s and the number of harmonics to compute n that should be avoided. The values of ρ_s to avoid for a given number of harmonics considered can be expressed as:

$$\rho_s = \frac{j}{i}; \quad i = 1, ..., n \text{ and } j = 0, ..., i \qquad (10)$$

which will make the matrix B non invertible.

Therefore, if we consider for example $n = 2$, the values of ρ_s which would lead to an ill-conditioned B matrix are: 0, 1 and 1/2, but if we consider $n = 3$ instead the values 1/3 and 2/3 are added to this list.

A representation of the condition number $\kappa(B)$ for all the range of ρ_s and considering several harmonics n is presented in Figure 4, where it can be seen that by increasing the number of harmonics the new critical set of values for ρ_s includes the precedents. In addition, values of ρ_s closer to the ones described by equation (10) will also result in an ill-conditioned matrix B. This result shows that some oscillations are only suitable to identify until a certain number of points in the frequency domain.

Local minima for $\kappa(B)$ are found approximatively in the middle between the values to avoid and the absolute minimal values are found at the origin and at $\rho_s = 1$. Intuitively, it can be seen that:

$$\lim_{\rho_s \to 0} \sin(n\pi\rho_s) \approx \rho_s,$$

which leads approximatively to an identity matrix multiplied by ρ_s.

With $\kappa(B)$ already characterized, the study of the condition number of A can be addressed. Regarding to matrix A the arguments of the sinusoidal functions can be rewritten using the following expression for the sake of simplicity:

$$2\tau_i - \rho_s = \theta_i, \qquad (11)$$

simplifying the analysis.

3.2 Characterizing $\kappa(A)$

Regarding to the condition number $\kappa(A)$, it can be obtained as:

$$\kappa(A) = \frac{\sigma_{max}(A)}{\sigma_{min}(A)} \qquad (12)$$

where $\sigma_{max}(A)$ and $\sigma_{min}(A)$ are maximal and minimal singular values of A respectively, which can be calculated as the square root of the eigenvalues of the matrix AA^T, which can be defined with the following expression:

$$(AA^T)_{i,j} = \sum_{\eta=1}^{n} \cos(\eta\pi(\theta_i - \theta_j)) \qquad (13)$$

This matrix has some characteristics which can be spotted immediately, which are that the elements of the main diagonal are equal to n since $\cos(0) = 1$, and that $(AA^T)_{i,j} = (AA^T)_{j,i}$ since $\cos(\alpha) = \cos(-\alpha)$.

In order to make $\kappa(A)$ the minimum possible, which would be $\kappa(A) = 1$, and since all the elements of the main diagonal are the same, the minimum for $\kappa(A)$ would be

obtained by making all the elements outside the main diagonal of AA^T equal to 0:

$$(AA^T)_{i,j} = \sum_{\eta=1}^{n} \cos(\eta\pi(\theta_i - \theta_j)) = 0; \quad i \neq j \tag{14}$$

which developed can be expressed in a compact form as in equation (15). Keeping in mind that $\theta_j - \theta_i \neq 2k$, $k \in \mathbb{Z}$, the general solution to equation (15) is given by:

$$\theta_j - \theta_i = \begin{cases} \dfrac{2k}{n} \\ \\ \dfrac{2k-1}{n+1} \end{cases}, \quad k \in \mathbb{Z} \tag{16}$$

Despite the wide range of possible solutions given by the parameter k, for simplicity, only those that keep $\theta \in [0, 2]$ will be considered. This is due to the fact that the samples τ are taken in a single oscillation period, which implies $\tau_i \in [0, 1]$. Besides, the commutation time fraction $\rho_s \in]0, 1[$, and using expression (11) would imply that $\theta \in]-1, 3[$, however, the effect of ρ_s will be proven to be negligible, therefore, we will only consider $\theta \in [0, 2]$.

From these solutions it has been found that: 1) It is not possible to make all the elements outside the main diagonal equal to 0, 2) There exist several combinations of (θ_i, θ_j) that make the element $(AA^T)_{i,j} = 0$ and 3) the maximum set of phases $\{\theta_1, \theta_2, ..., \theta_k\}$ that make $(AA^T)_{i,j} = 0$, $i \leq k$, $j \leq k$ has size n and correspond to those that fulfill (see Appendix B):

$$\theta_k = \frac{2k}{n} + \mathcal{O}; \quad k = 0, ..., n-1 \ , \ \mathcal{O} \in \left[0, \frac{2}{n}\right] \tag{17}$$

This set of phases will be used for the calculus of $\kappa(A)$. Any lag $\mathcal{O}$ could be used for the calculations, but for the sake of simplicity consider $\mathcal{O} = 0$.

With this set of phases half of the required values for θ have been covered. Let us consider that to cover the remaining n values, the same set of phases is considered but adding a constant phase lag ψ resulting in:

$$\theta_k = \begin{cases} \dfrac{2(k-1)}{n} & \text{if} \quad k = 1, ..., n \\ \\ \dfrac{2(k-n-1)}{n} + \psi & \text{if} \quad k = n+1, ..., 2n \end{cases}, \tag{18}$$

leading to a simple set of phases defined by the index k and the phase lag ψ.

By using these phases, the resulting matrix AA^T can be expressed as a block matrix which facilitates computing the characteristic polynomial p_λ, which has the expression presented in equation (19), calculations detailed in Appendix C.

From this expression, the eigenvalues of AA^T are obtained, which are:

$$\lambda = n \pm n\cos(n\pi\psi), \quad \lambda = n \pm n\cos\left(\frac{n\pi}{2}\psi\right)$$

Computing the square root of the ratio between the maximum and the minimum of these eigenvalues results in the condition number of A. The minimum among all the possible values has been found to be $\kappa(A) = \sqrt{3}$, and is obtained for the values of θ_k presented in equation (18) considering a phase lag of $\psi = \dfrac{2}{3n}$.

Remark 1 *If the choice of the values θ_k is increased by a given constant $\mathcal{O} \in \Re$ such as that:*

$$\theta'_k = \theta_k + \mathcal{O}, \quad \forall k$$

the resulting condition number will be the same $\kappa(A) = \kappa(A')$. Note that by construction, using the expression (13), matrices $(A')(A')^T$ and AA^T are equivalent since the constant $\mathcal{O}$ is canceled:

$$((A')(A')^T)_{i,j} = \sum_{\eta=1}^{n} \cos(\eta\pi(\theta'_i - \theta'_j)) = \sum_{\eta=1}^{n} \cos(\eta\pi(\theta_i - \theta_j)) = (AA^T)_{i,j}$$

resulting in the same eigenvalues that those of AA^T, and therefore in the same condition number. This can be useful in those cases where some of the collected data is known to be corrupted, which allows selecting other data for the identification.

With the set of phases obtained in equation (18) together with the results presented in Remark 1, the samples can be taken at time fractions $\tau_k = (\theta'_k + \rho_s)/2$, where $\theta'_k = \theta_k - \rho_s$, and θ_k being obtained directly from equation (18), resulting in:

$$\tau_k = \begin{cases} \dfrac{k-1}{n} & \text{if} \quad k = 1, ..., n \\ \\ \dfrac{k-n-1}{n} + \dfrac{1}{3n} & \text{if} \quad k = n+1, ..., 2n \end{cases}, \tag{20}$$

matching the first sample with the upwards switch of the relay.

For several values of n, a summary of the corresponding time fractions τ_k according to expression (20) is presented in Table 1.

$$(AA^T)_{i,j} = \csc\left(\frac{\pi}{2}(\theta_j - \theta_i)\right)\sin\left(\frac{n\pi}{2}(\theta_j - \theta_i)\right)\cos\left(\frac{(n+1)\pi}{2}(\theta_j - \theta_i)\right) = 0; \quad \theta_j - \theta_i \neq 2k,\ k \in \mathbb{Z} \tag{15}$$

$$p_\lambda(AA^T) = \det(AA^T - \lambda I) = \left((n-\lambda)^2 - n^2\cos^2(n\pi\psi)\right)\left((n-\lambda)^2 - n^2\cos^2\left(\frac{n\pi\psi}{2}\right)\right)^{n-1} \tag{19}$$

Table 1
Summary of τ_k values leading to $\kappa(A) = \sqrt{3}$ as a function of the number of harmonics considered.

n	τ_1	τ_2	τ_3	τ_4	τ_5	τ_6	τ_7	τ_8	τ_9	τ_{10}	τ_{11}	τ_{12}
2	0	1/2	1/6	2/3								
3	0	1/3	2/3	1/9	4/9	7/9						
4	0	1/4	1/2	3/4	1/12	1/3	7/12	5/6				
5	0	1/5	2/5	3/5	4/15	1/15	4/15	7/15	2/3	13/15		
6	0	1/6	1/3	1/2	2/3	5/6	1/18	2/9	7/18	5/9	13/18	8/9

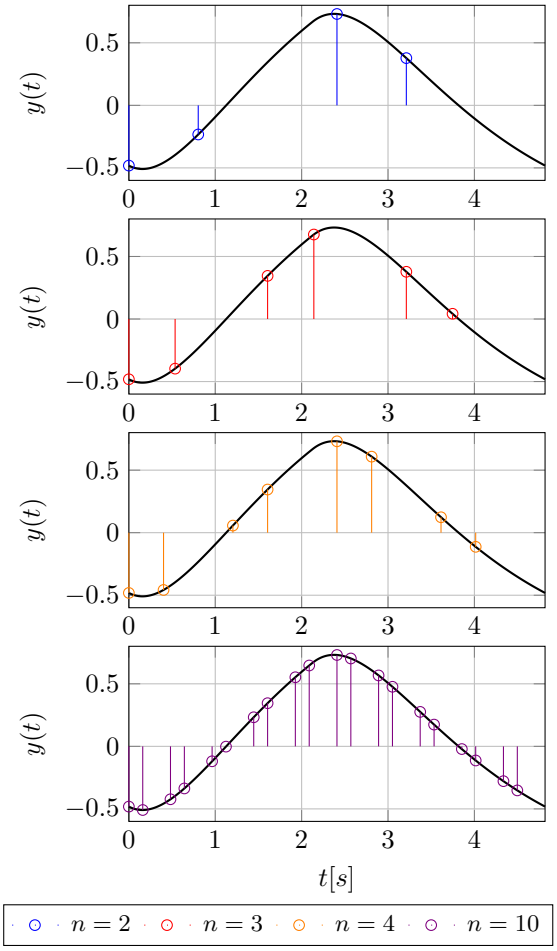

Fig. 5. Oscillation waveform resulting from a given asymmetric relay feedback experiment and an example of the samples taken depending on the number of harmonics.

In Figure 5 an oscillation generated by an asymmetric relay feedback experiment is presented together with the samples $y(\tau_k T_o)$ that should be taken to perform the identification according to the presented results for different number of harmonics.

It is worth noting that unlike standard frequency response identification methods, the approach proposed in this paper does not lie on estimating the Fourier Transform (FT) of sampled signals. Instead, the points of the frequency response are calculated straightforward by Fourier series using some properly selected samples of the oscillatory response obtained from a relay feedback experiment. Therefore, some undesired effects associated with the calculation of the FT of finite series, which result from the convolution of the spectrum of both the sampled signal and the measurement window, do not appear in our proposal. Similarly, the effect of the boundary conditions, i.e. the values at the beginning and at end of the experiment, which must be taken in account in standard frequency domain identification methods as a consequence of applying the Laplace transform to obtain a frequency domain model, [24], does not affect the results of the proposed procedure since such models are not used. In the approach presented in this paper the results are perturbed by both, the truncation of the Fourier series that approximate the temporal response of the system under oscillation and by the measurement error in signal y. The effects of these sources of estimation error will be analyzed in next sections.

4 Identification examples

In order to demonstrate the applicability of the proposed method, some identification examples are performed using as process to identify the models presented in (21)-(22), which contain some of the most common dynamics encountered in industrial processes.

$$G_1(s) = \frac{e^{-s}}{2s+1}$$

$$G_2(s) = \frac{e^{-s}}{(2s+1)^2} \tag{21}$$

$$G_3(s) = \frac{1}{(s+1)(0.1s+1)^2}$$

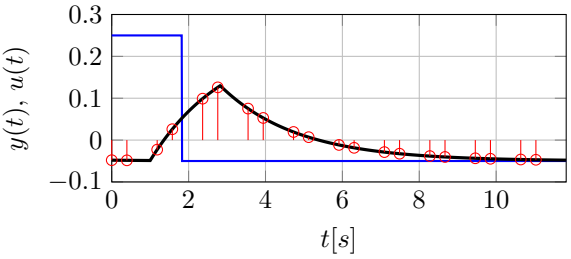

Fig. 6. Signals $u(t)$ and $y(t)$ for the system $G_1(s)$ used for identification: $y(t)$ in black, $u(t)$ in blue and samples at time fractions τ_k in red.

$$G_4(s) = \frac{1}{(s+1)^5}$$

$$G_5(s) = \frac{1}{(1+s)(1+0.5s)(1+0.5^2s)(1+0.5^3s)}$$

$$G_6(s) = \frac{e^{-0.3s}}{(1+s)(1+0.7s)} \tag{22}$$

$$G_7(s) = \frac{1-0.5s}{(s+1)^3}$$

$$G_8(s) = \frac{1}{(s+1)((0.5s)^2+0.7s+1)}$$

For the experiments consider the choice of the asymmetric relay parameters to be: $u_A = 0.25, u_B = -0.05, e_A = 0.548, e_B = 0.448$, and the reference to excite the systems is set to $y_r(t) = 0.5$. For the calculations, it has been considered the first 10 harmonics. Then, the time fractions τ_k have been chosen according to expression (20).

For each of the processes an experiment has been carried out and the corresponding data has been gathered. For example, for the process $G_1(s)$ the resulting oscillations for the proposed set-up has been presented in Figure 6, where $y(t)$ is presented in black, $u(t)$ in blue and the samples taken for the identification in red.

Using these data, ρ_s has been computed and matrices A and B calculated, allowing the estimation of the frequency response points for each system, gathered in the column vector S. As an example, the identification results obtained for system $G_1(s)$ are shown in Figure 7, in which the frequency response of the system in the Nyquist diagram has been presented in black, the points to identify, which correspond to the oscillation harmonics, are presented with black dots and the identified points in red. As it can be seen, the method results in an accurate estimation for the first points, specially considering that only 10 harmonics have been used. For the last harmonics, which are not presented in the figure, an estimation has also been computed using the method, however, is not as accurate, presenting in some cases a

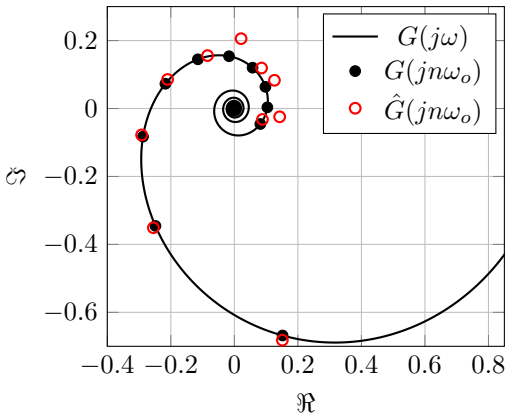

Fig. 7. Frequency response of system $G_1(s)$ in black, with the target points to estimate in black dots and the estimation in red.

Table 2
Relative error on the estimation for each model and harmonic considering $n = 10$.

	$\mathbf{Err_1}$	$\mathbf{Err_2}$	$\mathbf{Err_3}$	$\mathbf{Err_4}$	$\mathbf{Err_5}$
$\mathbf{G_1(s)}$	2.01	1.96	2.23	6.28	17.503
$\mathbf{G_2(s)}$	0.16	0.75	1.92	3.67	2.17
$\mathbf{G_3(s)}$	0.73	1.17	1.68	2.41	4
$\mathbf{G_4(s)}$	0.003	0.015	0.012	1.05	0.692
$\mathbf{G_5(s)}$	0.013	0.103	0.31	0.71	1.297
$\mathbf{G_6(s)}$	0.124	0.241	1.299	4.202	17.22
$\mathbf{G_7(s)}$	0.291	0.505	0.203	4.502	20.672
$\mathbf{G_8(s)}$	0.017	0.042	0.452	1.341	10.573

notable variation.

To quantify numerically the accuracy of the identification the parameter Err_n has been used, defined as:

$$Err_n[\%] = \frac{\left|G(jn\omega_o) - \hat{G}(jn\omega_o)\right|}{|G(jn\omega_o)|} \cdot 100, \tag{23}$$

which represents the relative error on the estimation of the harmonic n. This measure has been used to compute the accuracy of the estimation of the first five harmonics for the different processes presented in (21)-(22), the results are gathered in Table 2. As it can be seen in this table, the presented case $G_1(s)$ results in the most inaccurate estimations among all the considered cases. However, for this case, the results indicate that estimations around $Err = 2\%$ are obtained for the first three harmonics, which graphically in Figure 7 it can be seen that it is a reasonable estimation.

The current estimation of the frequency response points can be improved by considering more harmonics. This is a straightforward conclusion from the Fourier series analysis, the more harmonics are considered, the better the shape of $y(t)$ is approximated, and therefore, the subsequent calculations are more accurate.

Table 3
Err for the first 5 points obtained for process $G_1(s)$ considering $n = 10$ and $n = 20$ and the subsequent improvement.

	$\mathbf{Err_1}$	$\mathbf{Err_2}$	$\mathbf{Err_3}$	$\mathbf{Err_4}$	$\mathbf{Err_5}$
$\mathbf{n = 10}$	2.01	1.96	2.23	6.28	17.503
$\mathbf{n = 20}$	0.43	1.06	1.92	2.93	4.02
Improvement	1.58	0.89	0.31	3.36	13.48

This can demonstrated using for example the process $G_1(s)$. Another identification of the frequency response points has been carried out using the same oscillation that is presented in Figure 6, but doubling the number of harmonics involved in the calculus for the identification instead. Taking this into account the values τ_k are selected according to expression (20) and the identification is repeated. The relative error Err_n for both identifications is presented in Table 3, where it can be seen that improvements on the estimation are made for each harmonic.

5 Measurement noise influence

By considering an asymmetric relay with hysteresis, as depicted in Figure 2, it is assumed that the commutation thresholds e_A and e_B are chosen properly to avoid commutations due to noise. However, even if these switches are avoided, noise still has an influence on the linear system of equations used defined by (4), specifically on the measures vector Y.

Naming as s_k the k-th element of solution vector S and as u a column vector with the magnitudes of the measured noise, the influence of the noise on the final solution $\tilde{s}_k$ can be determined by the following expression (see Appendix D):

$$\tilde{s}_k = s_k + \frac{\pi}{2(u_A - u_B)} u^T \left[\left(A^{-1}\right)^T\right]_{*,k} \left(B^{-1}\right)_{k,k} \quad (24)$$

where subindex $\left[\left(A^{-1}\right)^T\right]_{*,k}$ denotes the k-th column of the matrix $(A^{-1})^T$, $(B^{-1})_{k,k}$ the element (k,k) of matrix B^{-1} and vector u denotes the magnitudes of the measured noise for each sample.

$(B^{-1})_{*,*}$ is known and can be computed as:

$$B^{-1} = diag\left(\frac{1}{\sin(\pi\rho_s)}, ..., \frac{n}{\sin(n\pi\rho_s)}, \frac{1}{\sin(\pi\rho_s)}, ..., \frac{n}{\sin(n\pi\rho_s)}\right)$$

which indicates that the noise is amplified for higher order harmonics. In addition, oscillations with values of ρ_s near the ones indicated by equation (10) also amplify the noise contribution for certain solutions $\tilde{s}_k$.

As in practice, obtaining the vector u might not be possible, from the practical point of view it is desirable to minimize its effect on the estimated solution $\tilde{s}_k$, which can be achieved by increasing the difference between the relay drive levels $(u_A - u_B)$. Increasing this magnitude will also increase the magnitude of the oscillation while not affecting the measuring noise u, which can be understood as reducing the Signal-to-Noise Ratio (SNR). This effect can be seen in equation (24) where it appears the ratio $u^T/(u_A - u_B)$.

6 Least Squares approach

In the equation system presented in expression (4) the number of equations l was assumed equal to twice the number of harmonics considered $(2n)$, which kept matrix A square. However, regarding to that expression, more than $2n$ equations can be taken to determine n number of points of the frequency response, becoming then a Least Squares (LS) problem.

For the LS formulation, the question of how to select the samples in order to obtain the most accurate response can also be formulated. However, since in Section 3 it has been found a sampling pattern that already provides a good condition number for A, in this section, that sampling pattern will be evaluated for the LS approach.

In Section 3, the time samples τ_k to select where defined by expression (20). As it can be seen, that expression is written in terms of the number of harmonics to calculate, not in the number of equations that are involved, which ultimately define the number of time fractions τ_k to select. As in the LS approach the equation system is overdetermined, more equations are involved, therefore, the expression to obtain the time samples τ_k can be generalized as:

$$\tau_k = \begin{cases} \dfrac{2(k-1)}{l} & \text{if} \quad k = 1, ..., l/2 \\ \dfrac{2(k-1)-l}{l} + \dfrac{2}{3l} & \text{if} \quad k = l/2+1, ..., l \end{cases}, \quad (25)$$

which is equivalent to expression (20) when $l = 2n$. As it can be seen, the number of equations l is always an even number.

To test the influence of the selected samples on the conditioning of A, a simple experiment has been run in which $\kappa(A)$ has been computed for combinations of $l \in [4, 200]$ and $n \in [1, l/2\text{-}1]$, which are all LS cases. The sampling times τ_k have been chosen according to equation (25) for each case. The results are presented in Figure 8, in which the obtained values of $\kappa(A)$ have been presented for its respective l and n but under the form of n/l.

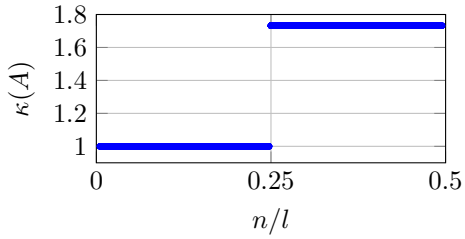

Fig. 8. Condition number of matrix A ($\kappa(A)$) obtained for combinations of $l \in [4, 200]$ and $n \in [1, l/2\text{-}1]$.

This simple experiment shows that by using the sampling pattern presented in equation (25), only two results are possible for the conditioning of A, which are either $\kappa(A) = 1$ or $\kappa(A) = \sqrt{3}$, this last being the value obtained for the square matrices case. The condition number improves ($\kappa(A) = 1$) for the cases in which $n/l < 1/4$, being only critical the conditioning of B which depends on the number of harmonics to identify n.

With regard to the condition number of B ($\kappa(B)$), as the size of this matrix depends exclusively on the number of harmonics to compute n, it remains as a square matrix, and then the same results obtained in Section 3 are applicable.

To compare LS approach with the square matrices approach described in Section 3 let us introduce the following example:

Example 2 *Consider a given process whose dynamics are described by the following model:*

$$G(s) = \frac{e^{-s}}{5s+1}.$$

For the relay setup consider $u_A = 1$, $u_B = -0.5$, $e_A = 0.488$ and $e_B = 0.188$. For the experiment, $y_r = 0$ has been used, and the resulting data collected. The first full oscillation obtained has been selected for identification and it can be seen in Figure 9, where it has been presented signals $u(t)$ in blue and $y(t)$ in black.

Let us consider that the first 6 harmonics are to be determined. To that end, to perform the identification three scenarios are presented. Firstly, a scenario where square matrices are used (as in Section 3) considering $l = 12$ and $n = 6$. Secondly, a scenario where the LS approach is followed considering $l = 50$ and $n = 6$. And finally, another scenario where the same number of equations as in the LS approach are used, but instead, square matrices will be employed, using $l = 50$ equations and computing $n = 25$ harmonics.

For each of these scenarios the samples τ_k are selected according to equation (25). For the first scenario, the samples τ_k have been highlighted in green on Figure 9 and, for the second and third scenarios, the corresponding samples τ_k have been represented in red in that figure. These samples together with the relay switch time fraction $\rho_s = 0.0968$ allow obtaining the matrix A for each case. Besides, matrix B is the same for the first two cases cases since both aim to determine the same amount of harmonics n, and bigger for the third case since n for that case is also bigger.

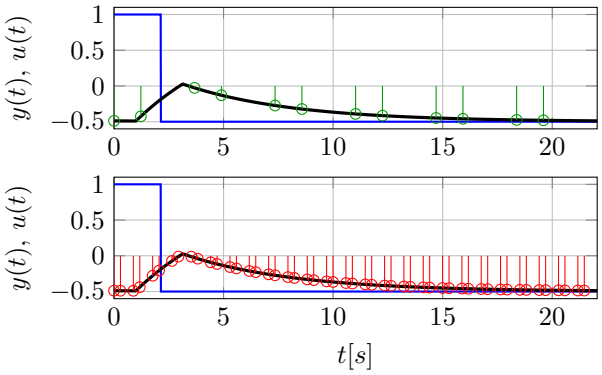

Fig. 9. Signals $u(t)$ and $y(t)$ for the system $G(s)$ used for identification: $y(t)$ in black, $u(t)$ in blue and samples at time fractions τ_k in green for $l = 12$ on top and in red for $l = 50$ below.

Table 4
Err for the first 6 harmonics according to each case: 1) square matrices with $l = 12$ and $n = 6$, 2) LS approach with $l = 50$ and $n = 6$, 3) square matrices with $l = 50$ and $n = 25$.

	$\mathbf{Err_1}$	$\mathbf{Err_2}$	$\mathbf{Err_3}$	$\mathbf{Err_4}$	$\mathbf{Err_5}$	$\mathbf{Err_6}$
Case 1	7.48	10.07	13.81	23.11	45.7	2.24
Case 2	0.43	0.68	0.79	0.66	0.63	2.21
Case 3	0.44	0.61	0.62	0.5	0.74	1.71

With all the data collected, the identification has been performed according to equation (4) to obtain the estimation of the frequency response points contained on the vector S. For the LS case the Moore-Penrose pseudo-inverse of matrix AB has been used. The resulting estimations are presented in Figure 10 for each case: the results for the first case are presented in green, for the second case in red and for the third case in orange. As it can be seen, the results obtained for the LS scenario are more precise than the ones obtained for the first scenario. In fact, they seem more similar to the results obtained for the third scenario. This is also reflected with the measure Err_n, which has been computed for the harmonics in common to the three cases, and it is presented in Table 4.

Therefore, despite not presenting exactly the same solution S for cases 2 and 3, the precision of their estimation is similar. This leads to think that accuracy in the estimation of the frequency response depends on the number of equations involved in the calculation. Thus, by using the LS approach an accuracy similar to the square matrices case, when using the same number of equations, is

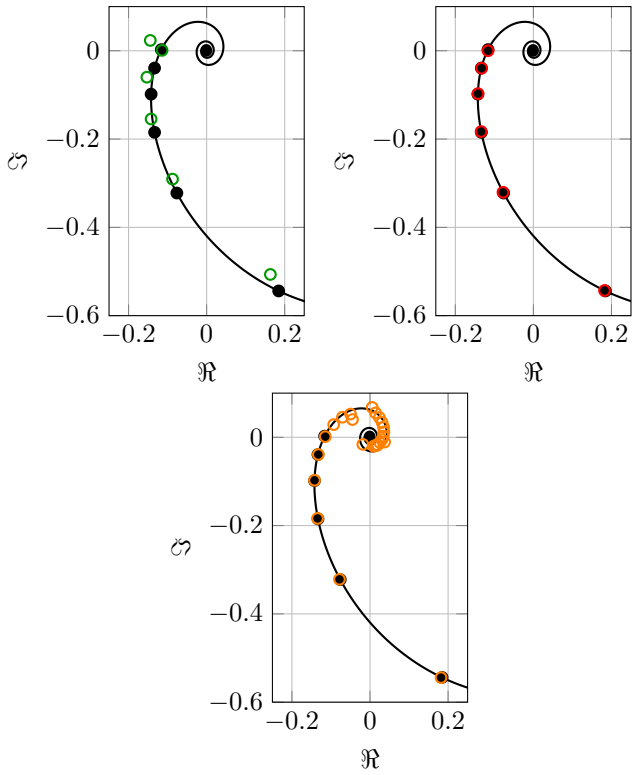

Fig. 10. Identification results: first case in green, square matrices with $l = 12$ and $n = 6$; second case in red, LS approach with $l = 50$ and $n = 6$; and third case in orange, square matrices with $l = 50$ and $n = 25$.

obtained for the harmonics in common.

Therefore, the usage of the LS approach, a priori, does not imply an improvement in the estimation of the harmonics with regard to the square matrices case with the same number of equations for the harmonics in common. This seems to be in contradiction with the condition number of the matrices involved, since for the square case, the condition number of matrix B is superior than for the LS case. Nevertheless, the condition number is related to the whole solution accuracy and does not reflect effectively the accuracy of the harmonics in common.

The main benefit of the LS approach is that it allows removing detrimental harmonics for the conditioning of B. Regarding to the results presented for matrix B in Section 3, as the number of harmonics n to compute increased, the number of values for ρ_s which made the matrix B singular increased. In the LS approach, the number of harmonics to calculate is lower than for the square matrices approach for the same accuracy, which reduces the number of critical values ρ_s to avoid. For example, if for a given experiment a value of $\rho_s = 1/9$ was obtained, with the square matrices approach we could only compute a maximum of $n = 8$ harmonics, with its associated accuracy, however, with the LS approach we can obtain those first 8 harmonics with a level of accuracy similar

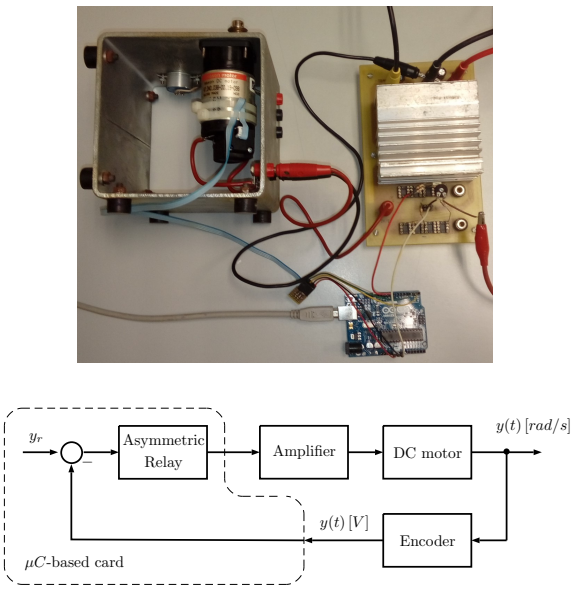

Fig. 11. Experimental setup and equivalent control loop.

to the one that would be obtained as if more harmonics were used in the square matrices case.

Besides, the meaningful region of the frequency response is described by the firsts harmonics, usually until a phase of $-180°$, which means that the rest of harmonics computed by the square matrices approach are less meaningful. Therefore, the usage of the LS approach does not present drawbacks in this sense, since the harmonics that are not computed are the least important.

7 Experimental case study

In this section, the principles proposed in this article are applied to a real case. It has been considered an experimental setup composed by a DC motor, which is regulated by an electronic card based on microprocessor, which is in charge of the data acquisition and of actuating on the system. This card actuates on the system using a PWM signal, which is then introduced into an electronic amplifier circuit which transforms it into the motor operation voltages for the motor regulation. The card displays as control output the mean tension of the PWM in the card's voltage scale, which ranges from 0V to 5V, which is then translated to the PWM duty cycle. The output of the motor is registered using an encoder, which allows computing the position and speed of the motor. The asymmetric relay for the identification is implemented in this card. The experimental setup and the equivalent loop are shown in Figure 11.

In this experiment the relationship between the speed of the motor and the mean tension to deliver will be characterized. For simplicity, only the measured voltage data will be used, but the real speed values in $[rad/s]$

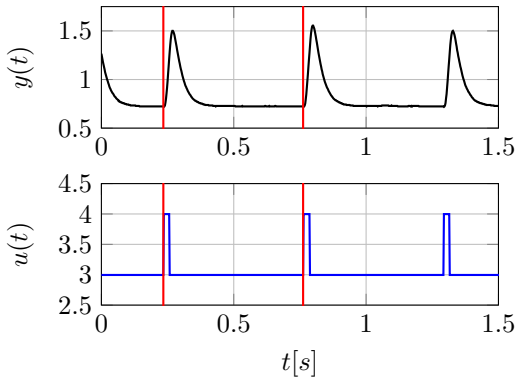

Fig. 12. Signals $y(t)$ and $u(t)$ from the experiment with the DC motor using an asymmetric relay. The first full cycle, delimited by red lines, is used to perform the identification.

can be obtained by multiplying the measured output y by the factor $204.6\,[rad/s]/[V]$.

For the experiment the parameters chosen for the asymmetric relay implemented in the electronic card have been chosen to be $u_A = 4, u_B = 3, e_A = 0.3, e_B = -0.25$ and the reference signal is set to maintain the controlled output $y(t)$ around 1, which will allow obtaining the motor frequency response in the surroundings of the operation point.

With the asymmetric relay configured an experiment has been performed, obtaining the signals $y(t)$ and $u(t)$ presented in Figure 12. This figure presents the collected data, however, only the first complete full cycle, which is delimited by two vertical red lines in both axis, is used for the identification procedure.

From the highlighted section of oscillations $y(t)$ and $u(t)$ the static gain of the process has been computed according to expression (3). Besides, the switch time fraction ρ_s and the oscillation period T_o have been measured resulting in $\rho_s = 0.0418$ and $T_o = 0.526\,s$.

For the identification two scenarios have been considered, one using square matrices and another one using the Least Squares approach. For the square matrices, $l = 200$ equations and $n = 100$ harmonics have been considered, and for the LS approach $n = 15$ harmonics using $l = 200$ equations. According to these scenarios, the samples to compute the identification have been selected according to the time fractions τ_k defined by expression (25). With all these data, the matrices A, B, Y and $\bar{Y}$ are constructed and the identification can be performed for both cases.

The results of both identifications are presented graphically in the Nyquist diagram in Figure 13. The results of identification when using square matrices are presented in red, and the results obtained for the LS approach in blue. For the square matrices approach, 100 points of the

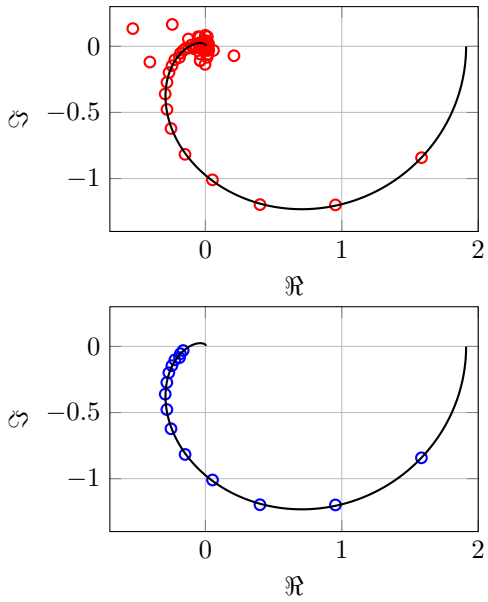

Fig. 13. Frequency response identification of DC motor transfer function. In red, square matrices approach with $l = 200$ and $n = 100$. In blue, LS approach with $l = 200$ and $n = 15$.

estimated frequency response $\hat{G}(jn\omega_o)$ are obtained, for the LS case only 15. For comparative purposes, an approximated theoretical transfer function has been presented in black in both figures.

Despite the overwhelming amount of points presented in the first case, not all of them present useful information. Graphically, it can be seen that some of them diverge significantly, and intuitively, as high harmonics are placed near the origin in the Nyquist diagram, a small variation in their estimation results in a high relative error.

8 Conclusions

In this paper, a methodology to obtain multiple frequency response points of systems using the information form a single asymmetric relay experiment has been proposed. The method uses the information from an induced oscillation to estimate the frequency response point related to the oscillation's period and a customizable number of harmonics. The accuracy on the estimation of each harmonic depends directly on the number of equations used, which is also an user-defined parameter. Besides, the proposal relies on the proper selection of the samples taken, which affect directly on the accuracy. Guidelines on how to select those samples are given. The method is applied to several processes which summarize some of the most common dynamics found in industry, showing that it can produce accurate results.

The proposal presented in this paper is a generalization of the standard relay feedback method which was originally developed to identify the ultimate point of the fre-

quency response used in auto-tunning algorithms of PID controllers. The new approach allows obtaining information of several points in a wide range of frequency without introducing variations in the experiment, keeping in that way its simplicity. Therefore, the proposed method can be useful to develop more sophisticated auto-tuning algorithms preserving the well known advantages of the relay feedback experiments.

The proposed method allows a Least Squares formulation, which has also been studied under the scope of the previously presented sample selection. The Least Squares approach allows obtaining accurate results using the same sample selection. In fact, the accuracy of the solution using a Least Squares approach is similar to the accuracy of the square matrices approach using the same number of equations for the harmonics in common. Furthermore, the Least Square approach can overcome one disadvantage of the method which is the critical switching time fraction ρ_s, producing more accurate results than the square matrices approach.

Finally, the proposed method has been applied to a real experimental case. Some points of the frequency response of a DC motor have been obtained using a single oscillation. The experiment shows the application of the proposed method using both the square matrices and the Least Squares approaches, validating experimentally their applicability and the accuracy in the estimation of both approaches for the harmonics in common.

Acknowledgements

This work was supported by Universitat Jaume I with grant number 18I411-Uji-b2018-39, MINECO with grant numbers DPI2017-84259-C2-2-R, RTI2018-094665-B-I00 and Ministerio de Ciencia e Innovación with grant number TEC2015-69155-R and by the State Research Agency under project PID2020-112658RBI00/10.13039/501100011033.

Appendix A Fourier series expansion of $\mathbf{y}(\tau\mathbf{T_o})$

Consider the signal $u(t)$ to be a square signal with pulse width modulated by ρ_s as shown in Figure 3, then the expression of $u(t)$ can be obtained through Fourier series expansion:

$$u(t) = \frac{a_0}{2} + \sum_{n=1}^{\infty} \Big(a_n \cos(n\omega_o t) + b_n \sin(n\omega_o t) \Big),$$

where a_0:

$$a_0 = \frac{2}{T_o} \int_0^{\rho_s T_o} u_A dt + \frac{2}{T_o} \int_{\rho_s T_o}^{T_o} u_B dt = 2\left(\rho_s \left(u_A - u_B\right) + u_B\right),$$

and a_n and b_n:

$$\begin{aligned} a_n =& \frac{2}{T_o} \int_0^{\rho_s T_o} u_A \cos(n\omega_o t) dt + \frac{2}{T_o} \int_{\rho_s T_o}^{T_o} u_B \cos(n\omega_o t) dt \\ =& \frac{1}{\pi n} (u_A - u_B) \sin(2\pi n \rho_s), \end{aligned}$$

$$\begin{aligned} b_n =& \frac{2}{T_o} \int_0^{\rho_s T_o} u_A \sin(n\omega_o t) dt + \frac{2}{T_o} \int_{\rho T_o}^{T_o} u_B \sin(n\omega_o t) dt \\ =& \frac{1}{\pi n} (u_A - u_B)(1 - \cos(2\pi n \rho_s)). \end{aligned}$$

Substituting:

$$\begin{aligned} u(t) =& \rho_s (u_A - u_B) + u_B + \\ & \sum_{n=1}^{\infty} \left(\frac{1}{\pi n} (u_A - u_B) \sin(2\pi n \rho_s) \cos(n\omega_o t) + \right. \\ & \left. \frac{1}{\pi n} (u_A - u_B)(1 - \cos(2\pi n \rho_s)) \sin(n\omega_o t) \right), \end{aligned}$$

$$\begin{aligned} u(t) =& \rho_s (u_A - u_B) + u_B + \frac{(u_A - u_B)}{\pi} \sum_{n=1}^{\infty} \frac{1}{n} \Big(\sin(n\omega_o t) \\ & + \sin(2\pi n \rho_s - n\omega_o t) \Big), \end{aligned}$$

$$\begin{aligned} u(t) =& \rho_s (u_A - u_B) + u_B + \\ & \frac{2(u_A - u_B)}{\pi} \sum_{n=1}^{\infty} \frac{1}{n} \sin(\pi n \rho_s) \cos(n\omega_o t - \pi n \rho_s) \end{aligned}$$

Expressing the time as a fraction of the oscillation period τT_o:

$$\begin{aligned} u(\tau T_o) =& \rho_s (u_A - u_B) + u_B + \\ & \frac{2(u_A - u_B)}{\pi} \sum_{n=1}^{\infty} \frac{1}{n} \sin(\pi n \rho_s) \cos(\pi n (2\tau - \rho_s)). \end{aligned}$$

Then, $y(t)$ is obtained by performing $y = G \cdot u$, where G is the open-loop transfer function of the system, which results in expression (26).

Appendix B Combination of solutions

The general solution of equation (15) is given by the following expression:

$$\theta_j - \theta_i = \begin{cases} \dfrac{2k}{n} \\ \\ \dfrac{2k-1}{n+1} \end{cases}, \quad k \in \mathbb{Z}$$

while avoiding $\theta_j - \theta_i = 2k$.

$$y(\tau T_o) = [\rho_s(u_A - u_B) + u_B]\, G(0) + \frac{2(u_A - u_B)}{\pi} \sum_{n=1}^{\infty} \frac{1}{n} \sin(\pi n \rho_s) \left[\Re\{G(j\omega_n)\} \cos(\pi n(2\tau - \rho_s)) - \Im\{G(j\omega_n)\} \sin(\pi n(2\tau - \rho_s))\right] \tag{26}$$

Due to the physical meaning of the phases, θ is comprised in a range from 0 to 2, therefore, the range of valid values for k must take this into account.

To test if the solutions for equation (15) can make all the elements outside the main diagonal of AA^T equal to 0 it must be tested for all the combinations of (i, j); $i \neq j$.

To facilitate this test, consider $\theta_1 = 0$, therefore, using the expression for the solution and applying the appropriate range for k and removing $\theta_{j\neq 1} = [0, 2]$, we have:

$$\theta_{j\neq 1} = \begin{cases} \left[\frac{2}{n}, ..., \frac{2(n-1)}{n}\right] \\ \left[\frac{1}{n+1}, \frac{3}{n+1}, ..., \frac{2n-1}{n+1}\right] \end{cases}.$$

Those are the values that should take the rest of θ_j to produce a 0 in the element $(AA^T)_{1,j}$. Note that there are $2n-1$ elements in that expression, which are the rest of phases θ.

Consider now that $\theta_2 = \frac{1}{n+1}$ and repeat the test to see if the phases θ coincide with those that θ_1 requires. In this case we should avoid $\theta_{j\neq 2} = \frac{1}{n+1}$, resulting in:

$$\theta_{j\neq 2} = \begin{cases} \left[\frac{1}{n+1} + \frac{2}{n}, ..., \frac{1}{n+1} + \frac{2(n-1)}{n}\right] \\ \left[0, \frac{2}{n+1}, ..., \frac{2n}{n+1}\right] \end{cases}.$$

As it can be seen the series $\theta_{j\neq 2}$ contains 0, which corresponds to θ_1, however, the rest of phases $\theta_{j\neq 2}$ that would make $(AA^T)_{2,j} = 0$ differ from those that are required by θ_1. Therefore, AA^T cannot be a diagonal matrix.

Until this point we have used for θ_2 the first element from the solution series for $\theta_{j\neq 1} = \left[\frac{1}{n+1}, \frac{3}{n+1}, ..., \frac{2n-1}{n+1}\right]$, but for the rest of the elements the same result is obtained.

Hence, consider now an element from the other solution series, for example $\theta_2 = 2/n$, applying the same procedure as before, omitting $\theta_{j\neq 2} = \frac{2}{n}$:

$$\theta_{j\neq 2} = \begin{cases} \left[0, \frac{4}{n}, \frac{6}{n}, ..., 2\right] \\ \left[\frac{2}{n} + \frac{-1}{n+1}, ..., \frac{2}{n} + \frac{2n-1}{n+1}\right] \end{cases}.$$

In this case, $\theta_{j\neq 2}$ also contains 0, which corresponds to θ_1, but some of the elements of the first series of phases: $\left[0, \frac{4}{n}, \frac{6}{n}, ..., 2\right]$, that make $(AA^T)_{2,j} = 0$, also belong to the first series of phases that would make $(AA^T)_{1,j} = 0$.

This test can be repeated for the values in common in both sets, and it would result in the same set of values repeating for each set excluding the one that is being tested. This can be seen regarding to the general expression of the solution set, the constraint $\theta_j - \theta_i = 2k/n$ has in the numerator an even number, thus, by adding and subtracting a multiple of the same form will result in another member of the same set. However, if we consider the elements resulting from the constraint $\theta_j - \theta_i = (2k-1)/(n+1)$ in the numerator there is an odd number, which added to another odd number makes an even number, falling outside the set. If that odd number is added to the even part of the solution, the resulting fraction cannot be simplified and therefore, it does not coincide with the other odd parts of the solution either.

These values constitute a larger set of solutions that the one tested before, specifically, if the previous test is repeated, it can be seen that the size of the set is n, and the elements that constitute it are:

$$\theta_k = \frac{2k}{n}; \quad k = 0, ..., n-1$$

Generalizing this expression by considering $\theta_1 \neq 0$ the same pattern is repeated, resulting in:

$$\theta_k = \frac{2k}{n} + \mathcal{O}; \quad k = 0, ..., n-1\ ,\ \mathcal{O} \in \left[0, \frac{2}{n}\right]$$

Appendix C Characteristic polynomial

Using the values of phase θ according to expression (18) matrix AA^T can be written as a block matrix as:

$$AA^T = \begin{bmatrix} \alpha & \beta \\ \gamma & \delta \end{bmatrix}$$

where every sub-matrix has size $n \times n$. The matrices involved can be expressed as:

$$\alpha = \delta = n \cdot I_{n\times n},$$

and β and γ as in expression (27).

The characteristic polynomial $p_\lambda(AA^T)$ is calculated as:

$$p_\lambda(AA^T) = \det(AA^T - \lambda I_{2n\times 2n}),$$

this does not change the elements in matrices β and γ, and only subtracts λ to the main diagonal of matrices α and δ, resulting in:

$$AA^T - \lambda I_{2n\times 2n} = \begin{bmatrix} \alpha' & \beta \\ \gamma & \delta' \end{bmatrix}, \quad \text{with} \quad \alpha' = \delta' = (n-\lambda) I_{n\times n}.$$

Since the presented blocks are square matrices and the product of γ and δ' fulfill the commutative property, the determinant can be computed as:

$$\begin{aligned} \det(AA^T - \lambda I_{2n\times 2n}) &= \det(\alpha'\delta' - \beta\gamma) \\ &= \det((n-\lambda)^2 I_{n\times n} - \beta\gamma), \end{aligned}$$

All the elements in the main diagonal of matrix $\beta\gamma$ are equal, which for simplicity will be referred to as a, the elements outside that diagonal are equal between them, and will be referred to as b:

$$(\beta\gamma)_{i,j} = \begin{cases} a & i = j \\ b & i \neq j \end{cases}$$

Thus, the determinant for the characteristic polynomial can be calculated as:

$$\begin{vmatrix} (n-\lambda)^2 - a & -b & -b & ... & -b \\ -b & (n-\lambda)^2 - a & -b & ... & -b \\ -b & -b & (n-\lambda)^2 - a & ... & -b \\ ... & ... & ... & & ... \\ -b & -b & -b & ... & (n-\lambda)^2 - a \end{vmatrix}.$$

Since applying linear operations between rows and columns does not alter the value of the determinant, we have subtracted to every row, except from the first one, the first one, see expression (28), and then added to the first column the other columns, see expression (29), resulting in a triangular matrix, therefore the determinant is the product of the elements in the main diagonal:

$$p_\lambda(AA^T) = \left((n-\lambda)^2 - a - b(n-1)\right)\left((n-\lambda)^2 - a + b\right)^{n-1}.$$

Using symbolic calculus manipulations from the expressions defining $(\beta\gamma)_{i,j}$ it has been obtained that:

$$\begin{cases} -a - b(n-1) = -n^2 \cos^2(n\pi\psi) \\ b - a = -n^2 \cos^2\left(\dfrac{n\pi\psi}{2}\right) \end{cases}$$

Resulting in the characteristic polynomial presented in expression (30).

Appendix D Noise influence calculation

The linear system presented in (4) can be expressed for simplicity as $b = \mathcal{A}S$ where $b = Y - \bar{Y}$, and $\mathcal{A} = \dfrac{2(u_A - u_B)}{\pi} AB$.

Let a measurement with noise $\tilde{b}$ be defined as $\tilde{b} = b + u$ where u denotes a vector with the noise magnitudes, then $\tilde{b} = \mathcal{A}\tilde{S}$. Solving by Cramer's rule:

$$\tilde{s}_k = \frac{\det(\mathcal{A}_k)}{|\mathcal{A}|},$$

where $\mathcal{A}_k$ is the matrix formed by replacing the k-th column of $\mathcal{A}$ by the column vector $\tilde{b}$. Developing:

$$\begin{aligned} \tilde{s}_k =& \frac{\det\left(\left[\mathcal{A}_{*,1\ldots k-1} \;\; b+u \;\; \mathcal{A}_{*,k+1\ldots 2n}\right]\right)}{|\mathcal{A}|} \\ =& \frac{\det\left(\left[\mathcal{A}_{*,1\ldots k-1} \;\; b \;\; \mathcal{A}_{*,k+1\ldots 2n}\right]\right)}{|\mathcal{A}|} \\ &+ \frac{\det\left(\left[\mathcal{A}_{*,1\ldots k-1} \;\; u \;\; \mathcal{A}_{*,k+1\ldots 2n}\right]\right)}{|\mathcal{A}|} \\ =& s_k + \frac{\det\left(\left[\mathcal{A}_{*,1\ldots k-1} \;\; u \;\; \mathcal{A}_{*,k+1\ldots 2n}\right]\right)}{|\mathcal{A}|} \end{aligned}$$

where $\mathcal{A}_{*,i\ldots j}$ denotes all the rows of columns from i to j. Second part of this expression can be further simplified by developing the determinant by the column k as the product of the vector u by the cofactor matrix of $\mathcal{A}$, $\text{cof}(\mathcal{A})$. Knowing that $\text{cof}(\mathcal{A}) = \text{adj}(\mathcal{A})^T$ and $|\mathcal{A}|\, A^{-1} = \text{adj}(\mathcal{A})$:

$$\tilde{s}_k = s_k + \frac{1}{|\mathcal{A}|} u^T \left[\left(|\mathcal{A}|\, \mathcal{A}^{-1}\right)^T\right]_{*,k} = s_k + u^T \left[\left(\mathcal{A}^{-1}\right)^T\right]_{*,k}$$

$$\beta_{i,j} = \gamma_{j,i} = \csc\left(\frac{\pi}{2}\left((j-i)\frac{2}{n}+\psi\right)\right)\sin\left(\frac{n\pi}{2}\left((j-i)\frac{2}{n}+\psi\right)\right)\cos\left(\frac{(n+1)\pi}{2}\left((j-i)\frac{2}{n}+\psi\right)\right) \tag{27}$$

$$\begin{vmatrix} (n-\lambda)^2-a & -b & -b & ... & -b \\ -b-(n-\lambda)^2+a & (n-\lambda)^2-a+b & 0 & ... & 0 \\ -b-(n-\lambda)^2+a & 0 & (n-\lambda)^2-a+b & ... & 0 \\ ... & ... & ... & & ... \\ -b-(n-\lambda)^2+a & 0 & 0 & ... & (n-\lambda)^2-a+b \end{vmatrix} \tag{28}$$

$$\begin{vmatrix} (n-\lambda)^2-a-b(n-1) & -b & -b & ... & -b \\ 0 & (n-\lambda)^2-a+b & 0 & ... & 0 \\ 0 & 0 & (n-\lambda)^2-a+b & ... & 0 \\ ... & ... & ... & & ... \\ 0 & 0 & 0 & ... & (n-\lambda)^2-a+b \end{vmatrix} \tag{29}$$

$$p_\lambda(AA^T) = \left((n-\lambda)^2 - n^2\cos^2(n\pi\psi)\right)\left((n-\lambda)^2 - n^2\cos^2\left(\frac{n\pi\psi}{2}\right)\right)^{n-1} \tag{30}$$

substituting $\mathcal{A}$, note that $B = B^T$ and that B is a diagonal matrix:

$$\tilde{s}_k = s_k + \frac{\pi}{2(u_A - u_B)} u^T \left[\left(A^{-1}\right)^T\right]_{*,k} \left(B^{-1}\right)_{k,k}$$

References

[1] Karl Johan Åström and Tore Hägglund. Automatic tuning of simple regulators with specifications on phase and amplitude margins. *Automatica*, 20(5):645–651, 1984.

[2] Josefin Berner, Tore Hägglund, and Karl Johan Åström. Asymmetric relay autotuning–practical features for industrial use. *Control Engineering Practice*, 54:231–245, 2016.

[3] Josefine Berner. Automatic tuning of PID controllers based on asymmetric relay beedback, 2015.

[4] Yu Jin Cheon, Chun Ho Jeon, Jietae Lee, Su Whan Sung, and Dong Hyun Lee. Improved fourier transform for processes with initial cyclic-steady-state. *AIChE journal*, 56(6):1536–1544, 2010.

[5] Yu Jin Cheon, Su Whan Sung, Jietae Lee, Cheol Ho Je, and In-Beum Lee. Improved frequency response model identification method for processes with initial cyclic-steady-state. *AIChE journal*, 57(12):3429–3435, 2011.

[6] Moisés T da Silva and Péricles R Barros. A robust relay feedback structure for processes under disturbances: Analysis and applications. *Journal of Control, Automation and Electrical Systems*, 30(6):850–863, 2019.

[7] Mats Friman and Kurt V Waller. A two-channel relay for autotuning. *Industrial & engineering chemistry research*, 36(7):2662–2671, 1997.

[8] Arthur Gelb and Wallace E. Van der Velde. *Multiple-input describing functions and non-linear system design*. McGraw-Hill, 1968.

[9] Milan Hofreiter. Shifting method for relay feedback identification. *IFAC-PapersOnLine*, 49(12):1933–1938, 2016.

[10] Ibrahim Kaya and Derek P. Atherton. Parameter estimation from relay autotuning with asymmetric limit cycle data. *Journal of Process Control*, 11(4):429–439, 2001.

[11] D Kishore, K Anand Kishore, and RC Panda. Identification and control of process using the modified asymmetrical relay feedback method. *Procedia computer science*, 133:1029–1034, 2018.

[12] RJ Kochenburger. Analyzing contactor servomechanisms by frequency-response methods. *Electrical Engineering*, 69(8):687–692, 1950.

[13] Nikolai Mitrofanovich Krylov and Nikolai Nikolaevich Bogoliubov. *Introduction to non-linear mechanics*. Princeton university press, 1949.

[14] Jietae Lee, Su Whan Sung, and Thomas F. Edgar. Integrals of relay feedback responses for extracting process information. *AIChE journal*, 53(9):2329–2338, 2007.

[15] Tong H. Lee, Qing-Guo Wang, and Kok Kiong Tan. A modified relay-based technique for improved critical point estimation in process control. *IEEE Transactions on Control Systems Technology*, 3(3):330–337, 1995.

[16] Alberto Leva, Luca Bascetta, and Francesco Schiavo. Model-based proportional- integral/proportional-integral- derivative (pi/pid) autotuning with fast relay identification. *Industrial & engineering chemistry research*, 45(12):4052–4062, 2006.

[17] Wei Li, Esref Eskinat, and William L Luyben. An improved autotune identification method. *Industrial & engineering chemistry research*, 30(7):1530–1541, 1991.

[18] Tao Liu and Furong Gao. *Industrial process identification and control design: step-test and relay-experiment-based methods*. Springer Science & Business Media, 2011.

[19] Tao Liu, Qing-Guo Wang, and Hsiao-Ping Huang. A tutorial review on process identification from step or relay feedback test. *Journal of Process control*, 23(10):1597–1623, 2013.

[20] Lennart Ljung. *System identification: theory for the user*. Prentice-hall, 1987.

[21] William L. Luyben. Getting more information from relay-feedback tests. *Industrial & engineering chemistry research*, 40(20):4391–4402, 2001.

[22] Oscar Miguel-Escrig and Julio-Ariel Romero-Pérez. Improving the identification from relay feedback experiments. *Automatica*, 135:109987, 2022.

[23] Rik Pintelon, Patrick Guillaume, Yves Rolain, Johan Schoukens, and Hugo Van Hamme. Parametric identification

of transfer functions in the frequency domain-a survey. *IEEE transactions on automatic control*, 39(11):2245–2260, 1994.

[24] Rik Pintelon and Johan Schoukens. *Appendix 6.B: Relation between DFT Spectra and Transfer Function for Arbitrary Signals*.

[25] Julio Ariel Romero, Roberto Sanchis, and Pedro Balaguer. PI and PID auto-tuning procedure based on simplified single parameter optimization. *Journal of Process Control*, 21(6):840–851, 2011.

[26] José Sánchez, Maria Guinaldo, Antonio Visioli, and Sebastián Dormido. Identification of process transfer function parameters in event-based pi control loops. *ISA transactions*, 75:157–171, 2018.

[27] José Sánchez Moreno, Sebastián Dormido, and José Manuel Díaz Martínez. Fitting of generic process models by an asymmetric short relay feedback experiment—the n-shifting method. *Applied Sciences*, 11(4):1651, 2021.

[28] José Sánchez Moreno, Sebastián Dormido, Oscar Miguel-Escrig, and Julio-Ariel Romero-Pérez. Asymmetric delayed relay feedback identification based on the n-shifting approach. *International Journal of Control*, pages 1–13, 2021.

[29] Roberto Sanchis, Julio A Romero, and Pedro Balaguer. Tuning of PID controllers based on simplified single parameter optimisation. *International Journal of Control*, 83(9):1785–1798, 2010.

[30] Claudio Scali, Gabriele Marchetti, and Daniele Semino. Relay with additional delay for identification and autotuning of completely unknown processes. *Industrial & engineering chemistry research*, 38(5):1987–1997, 1999.

[31] J. Schoukens, Y. Rolain, and R. Pintelon. Analysis of windowing/leakage effects in frequency response function measurements. *Automatica*, 42(1):27–38, 2006.

[32] Shih-Haur Shen, Jiun-Sheng Wu, and Cheng-Ching Yu. Use of biased-relay feedback for system identification. *AIChE Journal*, 42(4):1174–1180, 1996.

[33] Su Whan Sung, Jietae Lee, Dong Hyun Lee, Jong Hun Han, and Young Soo Park. Two-channel relay feedback method under static disturbances. *Industrial & engineering chemistry research*, 45(12):4071–4074, 2006.

[34] Su Whan Sung, Jin Hyun Park, and In-Beum Lee. Modified relay feedback method. *Industrial & engineering chemistry research*, 34(11):4133–4135, 1995.

[35] Kok K. Tan, Tong H. Lee, Sunan Huang, Kok Y. Chua, and Raihana Ferdous. Improved critical point estimation using a preload relay. *Journal of Process Control*, 16(5):445–455, 2006.

[36] T. Thyagarajan and Cheng-Ching Yu. Improved autotuning using the shape factor from relay feedback. *Industrial & engineering chemistry research*, 42(20):4425–4440, 2003.

[37] Qing-Guo Wang, Chang-Chick Hang, and Qiang Bi. Process frequency response estimation from relay feedback. *Control Engineering Practice*, 5(9):1293–1302, 1997.

[38] Qing-Guo Wang, Tong H. Lee, and Lin Chong. *Relay feedback: analysis, identification and control*. Springer Science & Business Media, 2012.

[39] Ya-Gang Wang and Hui-He Shao. Pid autotuner based on gain-and phase-margin specifications. *Industrial & engineering chemistry research*, 38(8):3007–3012, 1999.

[40] Cheng-Ching Yu. *Autotuning of PID Controllers. A Relay Feedback Approach*. Springer-Verlag London Limited, second edition.

Oscar Miguel-Escrig received the MS degree in Industrial Engineering from UJI Castelló and the MS degree in Automatics and Electronics Engineering from INSA Toulouse in 2017. In 2021 obtained the PhD in Industrial Technologies and Materials from UJI Castelló. His research interests include among others event-based control and automation in IEC 61499 standard.

Julio-Ariel Romero-Pérez received the BS and MS degrees in automatic engineering in 1995 and 1998 respectively from Universidad Central de las Villas in Cuba. In 2004 obtained the PhD in Automatic Control and Industrial Computing from UPV. Has been professor since 1995 in Universidad Central de las Villas and University Jaume I. His scientific activities include tuning and auto-tuning methods for industrial controllers, distributed control systems and event-based controllers.

José Sánchez-Moreno received the computer sciences degree in 1994 from UPM and the PhD degree in sciences from UNED in 2001. Since 1993 he has been a professor in UNED. His main research interests for the time being: event-based control, networked control systems, remote and virtual laboratories in control engineering, and pattern recognition in nuclear fusion databases.

Sebastián Dormido received the BS degree in physics from Madrid's Complutense University in 1968 and the PhD degree in the sciences from Basque Country University in 1971. He received a Doctor Honorary degree from the universities of Huelva and Almería. In 1981, he was appointed as a professor of control engineering at UNED. His scientific activities include computer control of industrial processes, model-based predictive control, and web-based labs for education. He has participated in more than 250 papers in international journals and conferences and has supervised more than 35 PhD thesis. He was the president of the Spanish Association of Automatic Control, CEA-IFAC. He received the National Automatic Control prize from IFAC Spanish Automatic Control Committee.